Biopathways Representation and Simulation on Hybrid Functional Petri Net

Hiroshi Matsuno[1], Yukiko Tanaka[1], Hitoshi Aoshima[1], Atsushi Doi[1], Mika Matsui[2], Satoru Miyano[3]

February 22, 2011

[1] Faculty of Science, Yamaguchi University, Japan
[2]Oshima National College of Maritime Technology
[3] Human Genome Center, Institute of Medical Science, University of Tokyo, Japan

Abstract

The following two matters should be resolved in order for biosimulation tools to be accepted by users in biology/medicine; (1) Remove issues which are irrelevant to biological importance, and (2) Allow users to represent biopathways intuitively and understand/manage easily the details of representation and simulation mechanism. From these criteria, we firstly define a novel notion of Petri net called *hybrid functional Petri net* (HFPN). Then, we introduce a software tool, *Genomic Object Net*, for representing and simulating biopathways, which we have developed by employing the architecture of HFPN.

In order to show the effectiveness of *Genomic Object Net* for representing and simulating biopathways, we show two HFPN representation of gene regulation mechanism of *Drosophila melanogaster* (fruit fly) circadian rhythm and apoptosis induced by Fas ligand. The simulation results of these biopathways are also presented with biological observations. The software is available to academic users from $http://www.GenomicObject.Net$.

1 Introduction

Considerable attentions have been paid to the biopathway representation and simulation in the literature. The most traditional approach is to employ ordinary differential equations (ODEs) such as Michaelis-Menten equations and to represent biochemical reactions as a systems of ODEs. This approach provides mathematically well-founded and fine interpretations of biopathways, especially for enzyme reactions. Gepasi [1] is a software package based on this approach for modeling biochemical systems and it aims at assisting users in translating reaction processes to matrices and ODEs. E-Cell [2] develops a system for representation and simulation with GUI and, with this tool, a model of a hypothetical cell with only 127 genes sufficient for transcription, translation, energy production and phospholipid synthesis is constructed.

As is stressed in [3] and [4], in order for software tools to be accepted by users in biology/medicine for biopathway modeling, we consider the following two matters should be resolved, at least: (1) Remove issues which are irrelevant to biological importance; Otherwise, users might be trained to understand some special notions in mathematics, physics and computer science which are irrelevant to biology/medicine. (2) Allow users to represent biopathways intuitively and understand/manage easily the details of representation and simulation mechanism; Otherwise, users could not have a confidence that the understanding and knowledge in their minds coincides with the object represented with the software tools.

From these criteria, in this paper, we firstly define a novel notion of Petri net called *hybrid functional Petri net* (HFPN) by extending the notions of hybrid Petri net [5] and functional Petri net [6] so that the notion will be suited for modeling biopathways.

Then, we introduce a software tool, *Genomic Object Net*, for representing and simulating biopathways, which we have developed by employing the architecture of HFPN. *Genomic Object Net* has an editor and a simulator of HFPN with GUI which shall resolve the matters (1) and (2). In order to demonstrate the effectiveness of *Genomic Object Net* for representing and simulating biopathways, we show a circadian rhythm of *Drosophila* as an example of gene regulatory mechanism and apoptosis induced by Fas ligand as an example of signal transduction.

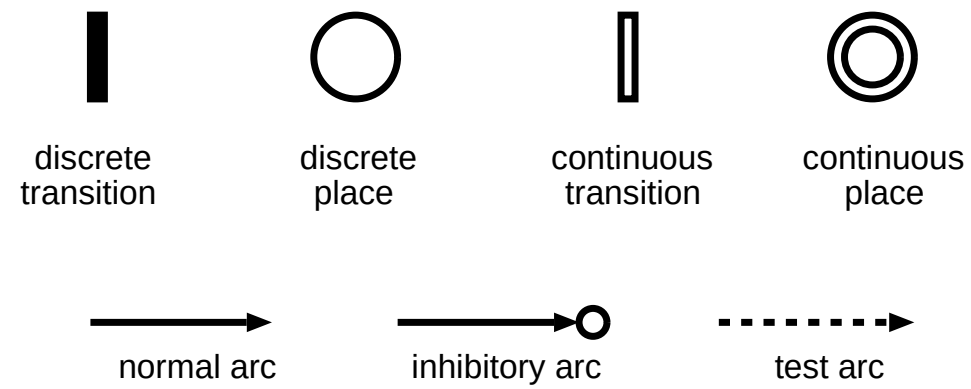

Figure 1: Elements of hybrid (functional) Petri net.

2 Hybrid Functional Petri Net

Ordinary differential equations (ODEs) are widely accepted to express biological phenomena such as biochemical reactions. But in this approach, it is rather difficult to observe the whole system intuitively like a picture if the system constitutes a large network of cascades. Although the discrete Petri net model allows very intuitive graphical representation, the mechanism of ODEs cannot be directly realized because the discrete Petri net model deals with only integers as the contents of places. For sophisticated dynamic systems in which control mechanisms of genes and chemical reactions with enzymes are concurrently performed, it is more reasonable to use real numbers for representing the amounts of some objects, e.g. the concentrations of a protein, mRNA, complex of proteins, metabolites, etc.

The hybrid Petri net model (HPN) [5] has been introduced as an extension of the discrete Petri net model so that it can handle real numbers in the continuous way and it allows us to express explicitly the relationship between continuous values and discrete values while keeping the good characteristics of discrete Petri net soundly. Drath [7, 8] has also enhanced this notion to define the hybrid dynamic net model (HDN) for modeling more complex systems.

In HPN/HDN model, two kinds of places and transitions are used, *discrete/continuous places* and *discrete / continuous transitions*. A discrete place and a discrete transition are the same notions as used in the discrete Petri net model. A continuous place holds a nonnegative real number as its content. A continuous transition fires continuously in the HPN/HDN model and its firing speed is given as a function of values in the places in the model. For graphical notations, discrete transition, discrete place, continuous transition and continuous place are drawn as shown in Figure 1.

From the definition of HPN/HDN, the firing speed of a continuous place must be the same as the consuming speed through each arc from its source place and the contents of all source places are consumed with the same speed. This speed is also the same as the production speed through each arc from the transition. This is the unfavorable feature of HPN/HDN for biopathway simulation. For example, consider a reaction in which a dimer is cleaved to two monomers (Figure 2 (a)). This reaction in the HDN model could be represented as shown in Figure 2 (b) by using a test arc and a transition for amplification (note that the amounts consumed and produced in places by continuous transition firing is the same by definition while the amount of monomers is twice as large as that of dimers). But it is neither intuitive nor natural at all. It may be obvious that this feature of HPN/HDN is a severe drawback in modeling biopathways.

On the other hand, some favorable features have been also introduced in Petri net theory. In addition to normal arc explained so far, *inhibitory arc* and *test arc* have been defined for convenience (Figure 1). An inhibitory arc with weight r enables the transition to fire only if the content of the place at the source of the arc is less than or equal to r. For example, an inhibitory arc can be used to represent the function of "repress" in gene regulation. A test arc does not consume any content of the place at the source of the arc by firing. For example, test arcs can be used to represent the transcription process since nothing is consumed by this process except for degradation.

Definition 1 A *hybrid functional Petri net* (HFPN) is defined by extending the notion of transition of HPN/HDN [5, 7, 8] in the following way: HFPN has five kinds of arcs; *discrete input arc*, *continuous input arc*, *test input arc*, *discrete output arc*, and *continuous output arc*. A discrete input arc (continuous input arc) is directed to

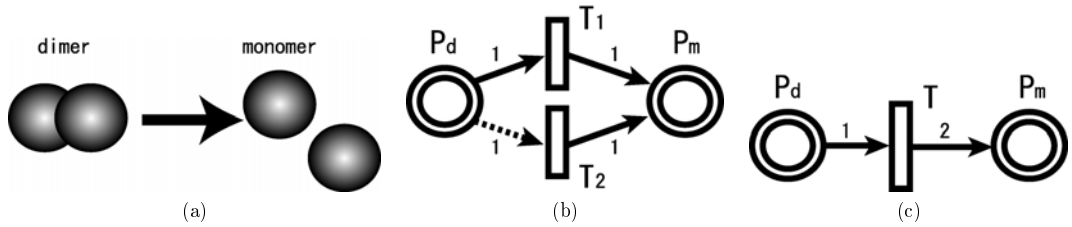

Figure 2: Models for reaction decomposing dimers to monomers. (a) Reaction decomposing dimers to monomers. (b) Hybrid Petri net model for the reaction. In continuous places $\mathrm{P_d}$ and $\mathrm{P_m}$, concentrations of the dimer and the monomer are stored, respectively. At continuous transitions $\mathrm{T_1}$ and $\mathrm{T_2}$, same firing speeds are assigned as the reaction speed. Integers "1" represent weights of arcs. (c) Hybrid functional Petri net model for the reaction. At the transition T, the reaction speed is assigned. $\mathrm{P_d}$ and $\mathrm{P_m}$ are the same as ones in (b). Different weights "1" and "2" are assigned to two arcs.

a discrete transition (continuous transition) from a discrete/continuous[1] place (continuous place) from which it consumes the content of the source place by firing. A test input arc is directed from a place of any kind to a transition of any kind. It does not consume the content of the source place. These three arcs are called *input arcs*. A discrete output arc is directed from a discrete transition to a place of any kind. A continuous output arc is directed from a continuous transition to a continuous place. These two arcs are called *output arcs*.

(1) Continuous transition: A *continuous transition* T of HFPN consists of continuous/test input arcs $a_1, \ldots, a_p$ from places $P_1, \ldots, P_p$ to T and continuous output arcs $b_1, \ldots, b_q$ from T to continuous places $Q_1, \ldots, Q_q$. Let $m_1(t), \ldots, m_p(t)$ and $n_1(t), \ldots, n_q(t)$ be the contents of $P_1, \ldots, P_p$ and $Q_1, \ldots, Q_q$ at time t, respectively. The continuous transition T specifies the following:

   (a) The *firing condition* is given by a predicate $c(m_1(t), \ldots, m_p(t))$. As long as this condition is true, T fires continuously.

   (b) For each input arc a_i, T specifies a function $f_i(m_1(t), \ldots, m_p(t)) \geq 0$ which defines the speed of consumption from P_i when it is firing. If a_i is a test input arc, then we assume $f_i \equiv 0$ and no amount is removed from P_i. Namely, $d[a_i](t)/dt = f_i(m_1(t), \ldots, m_p(t))$, where $[a_i](t)$ denotes the amount removed from P_i at time t through the continuous input arc a_i during the period of firing.

   (c) For each output arc b_j, T specifies a function $g_j(m_1(t), \ldots, m_p(t)) \geq 0$ which defines the speed of amount added to Q_j at time t through the continuous output arc b_j when it is firing. Namely, $d[b_j](t)/dt = g_j(m_1(t), \ldots, m_p(t))$, where $[b_j](t)$ denotes the amount of the contents added to Q_j at time t through the continuous output arc b_j during the period of firing.

(2) Discrete transition: A *discrete transition* T of HFPN consists of discrete/test input arcs $a_1, \ldots, a_p$ from places $P_1, \ldots, P_p$ to T and discrete output arcs $b_1, \ldots, b_q$ from T to places $Q_1, \ldots, Q_q$. Let $m_1(t), \ldots, m_p(t)$ and $n_1(t), \ldots, n_q(t)$ be the contents of $P_1, \ldots, P_p$ and $Q_1, \ldots, Q_q$ at time t, respectively. The discrete transition T specifies the following:

   (a) The *firing condition* is given by a predicate $c(m_1(t), \ldots, m_p(t))$. If this is true, T gets ready to fire.

   (b) The *delay function* given by a nonnegative integer valued function $d(m_1(t), \ldots, m_p(t))$. If the firing condition gets satisfied at time t, T fires in delay $d(m_1(t), \ldots, m_p(t))$. However, if the firing condition is changed during this delay time, the transition T looses the chance of firing and the firing condition will be reset.

   (c) For each input arc a_i, T specifies a nonnegative integer valued function $f_i(m_1(t), \ldots, m_p(t)) \geq 0$ which defines the the number of tokens (integer) removed from P_i through arc a_i by firing. If a_i is a test input arc, then we assume $f_i \equiv 0$ and no token is removed.

   (d) For each output arc b_j, T specifies a nonnegative integer valued function $g_j(m_1(t), \ldots, m_p(t)) \geq 0$ which defines the number of tokens (integer) are added to Q_j through arc b_j by firing.

In Figure 3, examples of continuous transition and discrete transition are shown.

[1] A/B means A or B.

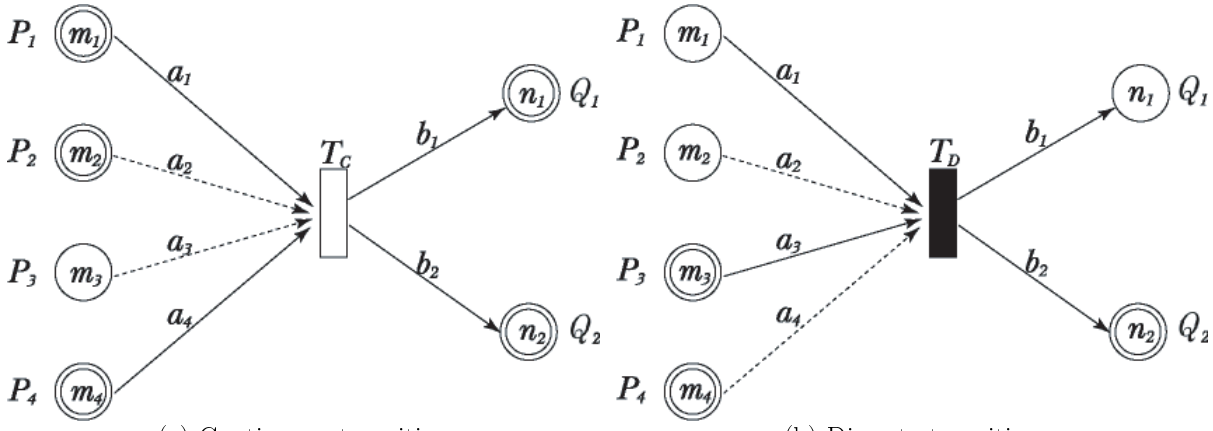

(a) Continuous transition (b) Discrete transition

Figure 3: Continuous and discrete transitions of hybrid functional Petri net. (a) An example of continuous transition. Four input arcs are attached to continuous transition T_C: two continuous input arcs from continuous places P_1 and P_4, and two test input arcs from continuous place P_2 and discrete place P_3. a_i is the weight of arc from place P_i for $i = 1, 2, 3, 4$. Two continuous arcs are headed from the transition T_C to continuous places Q_1 and Q_2, respectively. Variables b_1 and b_2 are assigned to these arcs as weights. (b) An example of discrete transition. Four input arcs are attached to discrete transition T_D: two discrete input arcs from discrete place P_1 and continuous place P_3, and two test input arcs from discrete place P_2 and continuous place P_4. a_i is the weight of arc from place P_i for $i = 1, 2, 3, 4$. Two output arcs are headed from the transition T_D to discrete place Q_1 and continuos place Q_2. Variables b_1 and b_2 are assigned to these arcs as weights.

From the above definition, it may be obvious that in the HFPN model, the dimer-to-monomers reaction can be intuitively represented as Figure 2 (c). Not only this simple example but also more complex interactions can be easily and intuitively described with HFPN. The software *Genomic Object Net* is developed and implemented based on this HFPN architecture.

3 Circadian Rhythms in *Drosophila*

The control mechanism of autoregulatory feedback loops of *Drosophila* circadian rhythms has been intensively studied [9, 10, 11, 12, 13, 16] and some fine modelings by ODEs with detailed coefficients have also been reported [14, 15]. These ODE-based models can be easily described with HFPNs with *Genomic Object Net*. Highly appreciating such fine modelings, we first show an HFPN realization of the model due to Ueda et al. [15]. Moreover, we also show that an HFPN can be designed with *Genomic Object Net* easily and intuitively by interpreting the biological facts and observations given in [9, 10, 11, 12, 13, 16]. *Genomic Object Net* is intended to be a naïve platform where we can create hypotheses and evaluate them by simulation. This feature is especially important when only rough modeling is enough or enough information is not available for fine modeling.

Figure 4 shows the scheme of the regulatory mechanism of five genes contributing to the *Drosophila* circadian rhythms; *period* (*per*), *timeless* (*tim*), *Drosophila Clock* (*dClk*), *cycle* (*cyc*) and *double-time* (*dbt*). It is known that the *Drosophila* circadian feedback system is composed of two interlocked negative feedback loops [10]. Roughly speaking, PER and TIM proteins collaborate in the regulation of their own expression in *Drosophila*, assembling in PER-TIM complexes that permit nuclear translocation, inactivation of *per* and *tim* transcription in a cycling negative feedback loop, and activation of *dClk* transcription which participates in the dCLK-CYC negative feedback loop. The *dCLK* and *CYC* form heterodimers that activate *per* and *tim* transcriptions and inhibit *dClk* transcription. Among these five genes, three genes, *per*, *tim*, and *dClk*, are rhythmically expressed: *per* and *tim* mRNA levels begin to rise in the subjective day and to peak early in the subjective evening, and *dClk* mRNA level peaks late at night to early in the morning. Although *per* and *tim* mRNAs reach peak levels in the evening, PER and TIM levels do not peak until late evening. It is considered that this delay results from the initial destabilization of PER by DBT-dependent phosphorylation followed by the stabilization of PER by dimerization with TIM [12, 13]. The details of the mechanism are surveyed in [9, 11, 16].

Ueda et al. [15] have modeled the two interlocked negative feedback loop system [10] with ODEs and made

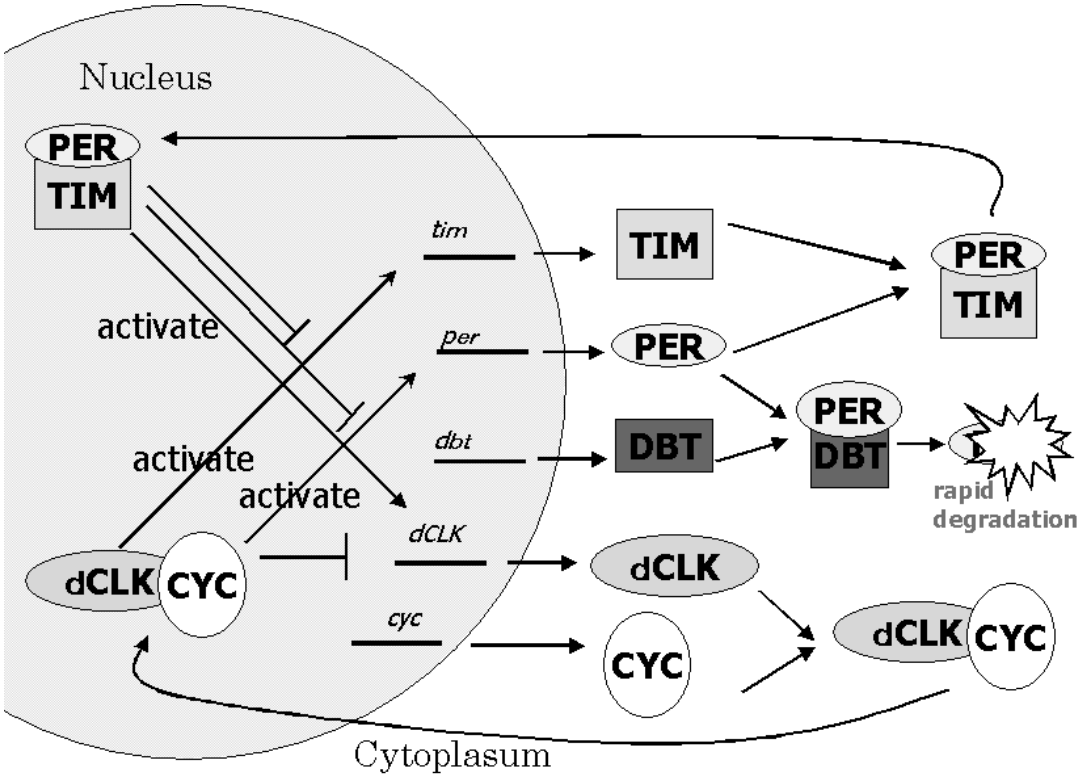

Figure 4: The gene regulation in the *Drosophila* circadian oscillator is schematized.

extensive simulation and mathematical analysis. We have translated it into an HFPN as in Figure 5 and further computational experiments based on this model are possible on *Genomic Object Net* with this HFPN file.

By using *Genomic Object Net*, we also designed an HFPN from scratch by interpreting the facts and observations in [9, 10, 11, 12, 13, 16]. Figure 6 is a naïve representation of the gene regulatory mechanism of *Drosophila* circadian oscillator, where continuous places are introduced and the functions for continuous transitions are defined and tuned so that the simulation results will coincide with the facts and observations. In Figure 6, smaller value of tokens $m2$ or $m4$ is taken as the complex forming rate of the proteins dCLK ($m2$) and CYC ($m4$) at the transition T_1. *Genomic Object Net* can assign a perl script to any transition for realizing such a sophisticated function. The following perl script of this case describes the program which takes smaller ones of tokens $m2$ or $m4$. The variable v represents the flow speed of the corresponding arc. In this case, to each of three arcs, dCLK $\rightarrow$ T_1, CYC $\rightarrow$ T_1, and T_1 $\rightarrow$ dCLK/CYC, the following perl script is assigned. Of course, different perl scripts can be assigned to the different arcs.

This example demonstrates the effectiveness of the HFPN architecture for representing biopathways. The firing speeds of these three transitions are changed according to the values in the places dCLK ($m2$) and CYC ($m4$).

```
if($m2>1 && $m4>1){
  if($m2<$m4){
    $v=$m2/20;
  }
  else{
    $v=$m4/20;
  }
}
else{
  $v=0;
}
```

Complex forming rates of PER/TIM and PER/DBT are similarly realized at the transitions T_2 and T_3, respectively, by using this function. Transitions T_4, T_5, and T_6 represent the degradation rates of complexes of

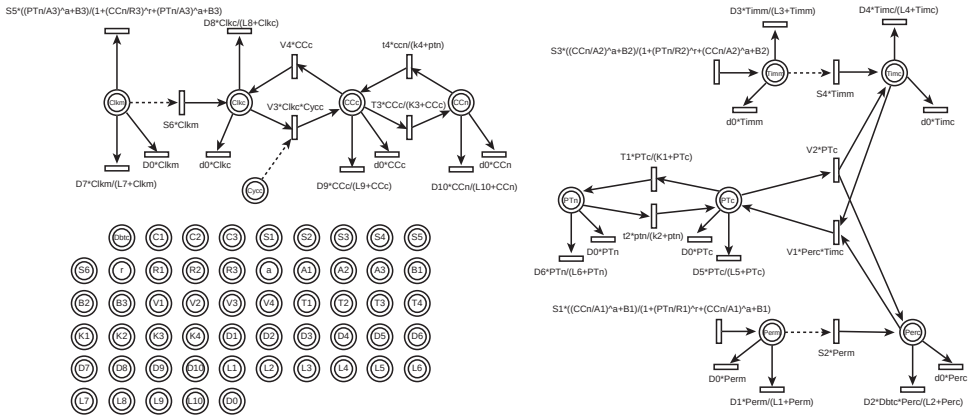

Figure 5: A HFPN realization of the circadian rhythm model due to Ueda et al. [15]. A series of ten ODEs, e.g. $\frac{dPer_m}{dt} = C_1 + S_1 \frac{\left(\frac{CC_n}{A_1}\right)^a + B_1}{1+\left(\frac{PT_n}{R_1}\right)^r + \left(\frac{CC_n}{A_1}\right)^a + B_1} - D_1 \frac{Per_m}{L_1 + Per_m} - D_0 Per_m$, are realized in this network, where Per_m (CC_n, PT_n) represents the concentration of *per* mRNA (dCLK-CYC complex in the nucleus, PER-TIM complex in the nucleus) and $C_1 = 0$nM/h, $S_1 = 1.4$nM/h, $A_1 = 0.45$nM/h, $B_1 = 0$, $L_1 = 0.3$nM/h, $D_0 = 0.012$nM/h, $D_1 = 0.94$nM/h, $R_1 = 1.02$nM/h.

the corresponding proteins. Figure 7 (a) is the simulation result of the HFPN in Figure 6. It indicates that this HFPN model representing two negative feedback loops, the PER-TIM feedback and the dCLK-CYC feedback, successfully produce periodic oscillations of *per* mRNA ($m6$), *tim* mRNA ($m8$), and *dClk* mRNA ($m1$), while the concentration of *cyc* mRNA ($m3$) keeps constant expression.

It is known that the protein TIM stabilizes phosphorylated PER by dimerizing with it. This phenomenon is reflected to the firing speed of transition T_5, that is, the firing speed of transition T_5 ($m13/15$) is set to be slower than the one of transition T_7 ($m7/10$). Moreover, it is suggested in [13] that the normal function of protein DBT is to reduce the stability and thus the level of accumulation of monomeric PER proteins. This function is realized in Figure 6 in transition T_3. It is clearly expressed in Figure 7 (b) that there is time difference around four hours between the peaks of concentrations of *per* mRNA and PER which is believed to be arisen from the above two facts. This indicates that the result of simulation is in good agreement with the experimental observation reviewed in [11].

4 Apoptosis Induced by Fas ligand

The purpose of this section is to show that *Genomic Object Net* based on HFPN is useful to model signal transduction pathways. We considered the biopathways known for the apoptosis induced by Fas ligand and made a computational experiment for evaluating the effect of autocatalytic process. In this HFPN modeling, we do not use the special function of perl script as is described in Section 3.

Apoptosis, programmed cell death, is known to participate in various biological processes such as development, maintenance of tissue homeostasis and elimination of cancer cells [17, 18]. Malfunctions of apoptosis have been implicated in many forms of human diseases such as neurodegenerative diseases, AIDS and ischemic stroke. Reportedly, apoptosis is caused by various inducers such as chemical compounds, proteins or removal of NGF. The biochemical pathways of apoptosis are complex and depend on both the cells and the inducers.

Fas-induced apoptosis has been studied in detail and its mechanism has been proposed as shown in Figure 9 [19]. Fas ligands, which usually exist as trimmers, bind and activate their receptors by inducing receptor trimerization. Activated receptors recruit adaptor molecules such as Fas-associating protein with death domain (FADD), which recruit procaspase 8 to the receptor complex, where it undergoes autocatalytic activation. Activated caspase 8 activates caspase 3 through two pathways; The complex one is that caspase 8 cleaves Bcl-2 interacting protein (Bid) and its COOH-terminal part translocates to mitochondria where it triggers cytochrome c release. The released cytochrome c bind to apoplectic protease activating factor-1 (Apaf-1) together with dATP and procaspase 9 and activates caspase 9. The caspase 9 cleaves procaspase 3 and activates caspase 3. The other pathway is that caspase 8 cleaves procaspase3 directly and activates it. The caspase 3 cleaves DNA fragmentation factor (DFF) 45 in a heterodimeric factor of DFF40 and DFF45. Cleaved DFF45 dissociates

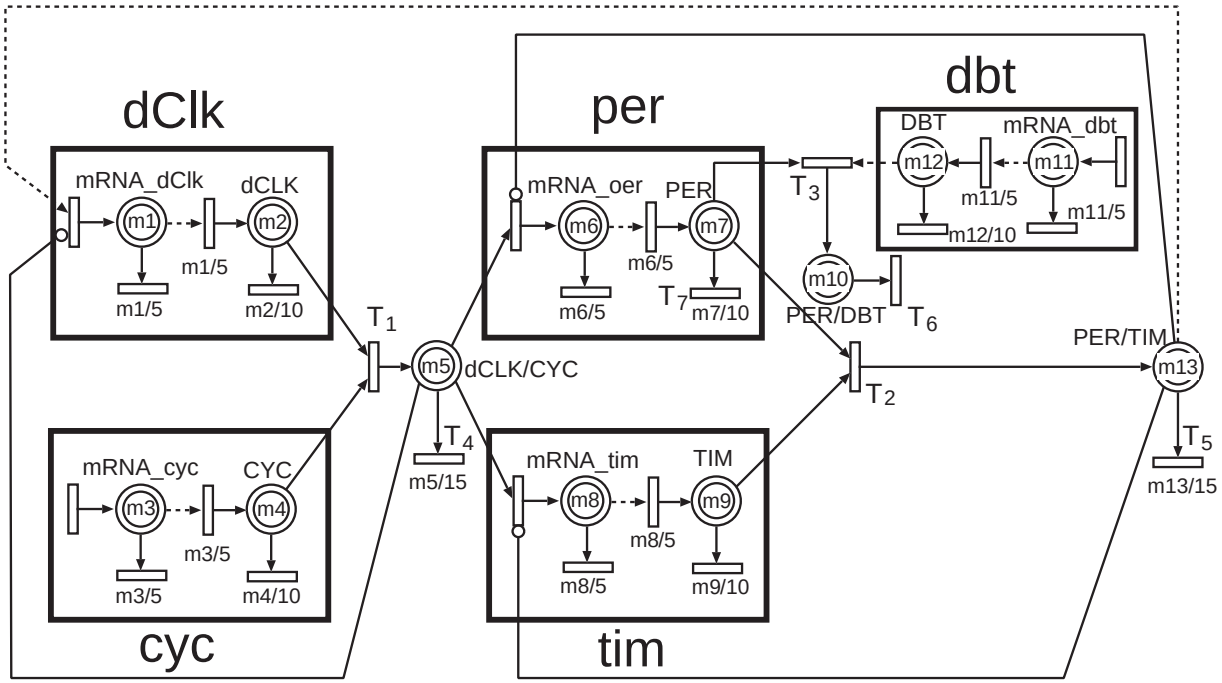

Figure 6: A naïve HFPN representation of *Drosophila* circadian mechanism in which five genes *per*, *tim*, *dClk*, *cyc*, and *dbt* participate. A HFPN file including all transition parameters can be downloaded from the URL $http://www.GenomicObject.Net$.

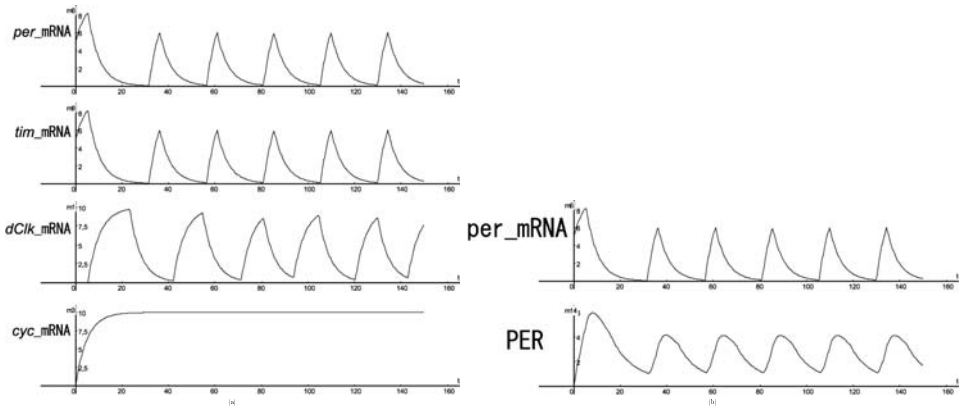

Figure 7: (a) Behaviors of concentrations of four mRNAs simulated on *Genomic Object Net*. (b) Time difference around four hours is observed between the peaks of concentrations of *per* mRNA and PER.

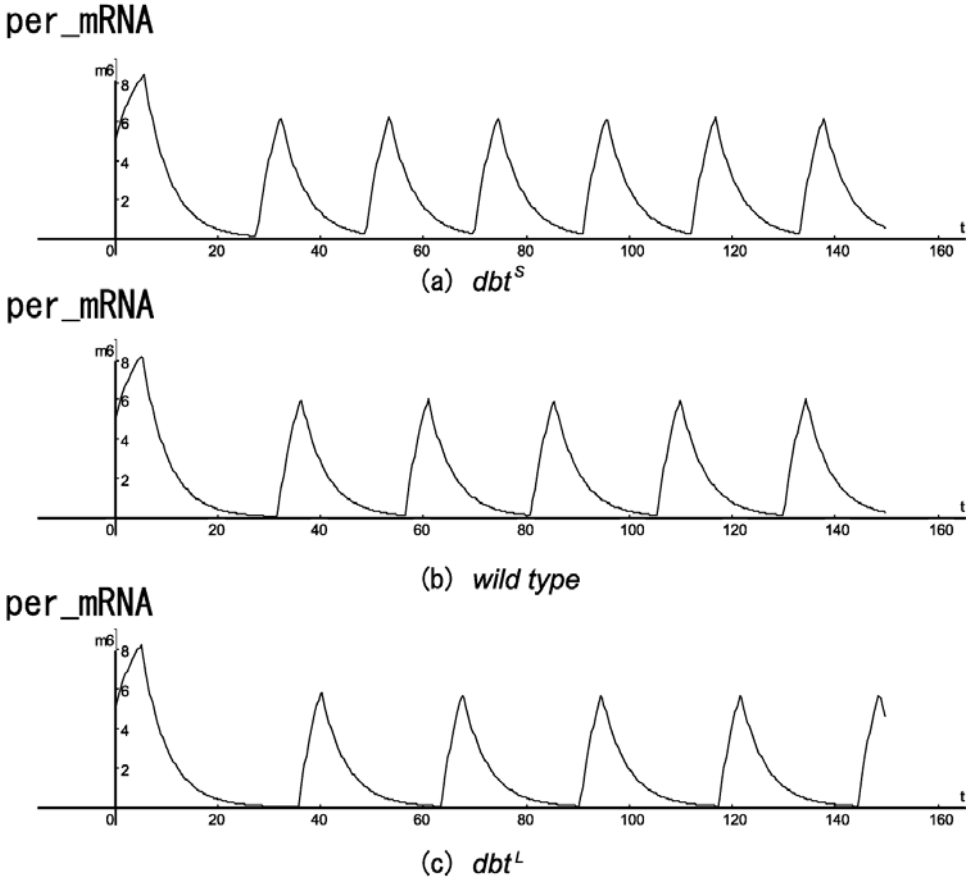

Figure 8: Concentration behaviors of *per* mRNA. (a) dbt^L mutant (b) Wild type (c) dbt^S mutant

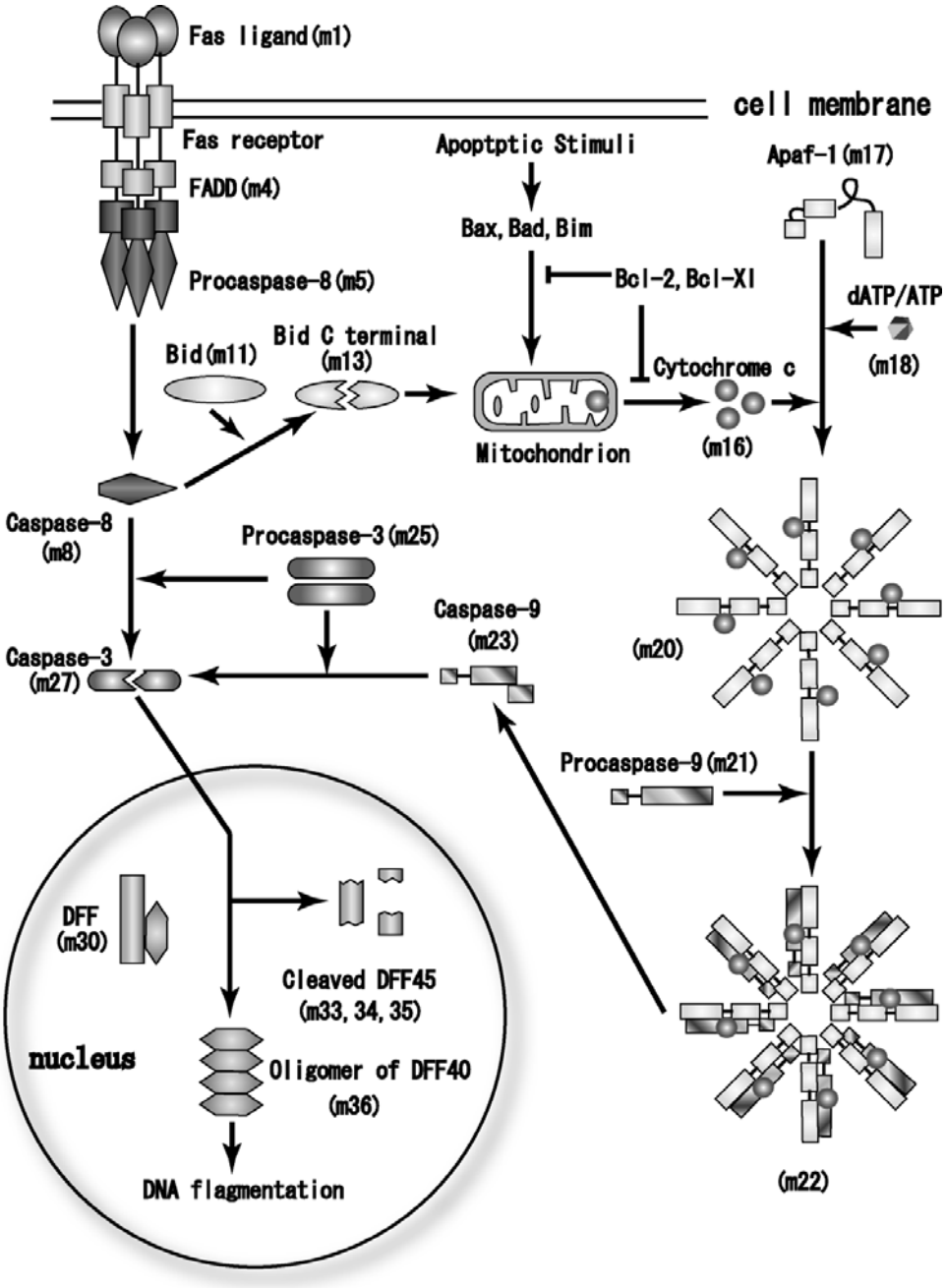

Figure 9: Proposed steps of apoptosis induced by Fas ligand.

Table 1: Functions assigned to continuous transitions in the simulation of apoptosis induced by Fas ligand, where mA and mB represent the contents of the corresponding continuous places.

Rate	Unimolecular reaction	Bimolecular reaction
Self-effacement	$mA/200$	
Oligomer	$mA/20$	$mA * mB/10000$
Monomer	$mA/10$	$mA * mB/5000$
Enzyme binding	$mA/5$	$mA * mB/2500$
Enzyme reaction	$mA * 10$	

from DFF40, inducing oligomerization of DFF40 that has DNase activity. The active DFF40 oligomer causes the internucleosomal DNA fragmentation, which is an apoptotic hallmark indicative of chromatin condensation.

We described this mechanism as a HFPN with *Genomic Object Net*. The pathways consist of several steps where two different pathways from caspase 8 are assumed and many molecules including Fas receptors, caspase family which includes aspartic acid-dependent cysteine proteases and produced from their zymogens, Bcl-2 family which includes pro- and anti-apoptotic proteins, cytochrome c and DNA fragmentation factor. The apoptosis starts from the Fas ligand binding to Fas receptors and ends in the fragmentation of genomic DNA, which is used as a hallmark of apoptosis. Thus the amount of DNA fragmentation can be assumed to be proportional to the cell death.

We have designed an HFPN by using the facts about the Fas-induced apoptosis pathways shown in Figure 9 and biochemical knowledge about reactions. Figure 10 shows the whole HFPN representation that we have described with *Genomic Object Net*. All places/transitions are continuous and parameters are roughly tuned by hands. For Bid ($m11$), Procaspase-9 ($m21$), Procaspase-3 ($m25$), DFF ($m30$), DNA ($m37$), the initial concentration of each compound is assumed to be 100. On the other hand, for FADD ($m4$), Procaspase-8 ($m5$), Apaf-1 ($m17$), dATP/ADP ($m18$), when two compounds react together without the stimulation of apoptosis, the initial concentrations and the rate are assumed to be 39.039 and $m1 * m2/5000$, respectively to keep the stable state condition. Each compound is assumed to be produced by the rate of 0.5 (represented by a transition without any incoming arc) and to degrade by the rate of its concentration divided by 200 (represented by a transition without any outgoing arc), which will keep its concentration at 100 under the stable state condition. This degradation rate also applies to other compounds in the network. The rate of other processes are determined roughly by following Table 4. Synthesis and catabolism processes are added in the model for all proteins. Autocatalytic processes are also added in the model to all caspases since they exist as proenzymes. The pathway from caspase 8 to caspase 3 is assumed when the caspase 8 concentration is over 30. Protease is often synthesized as a proenzyme (zymogen) and changed to active form by other enzymes or by itself. So autocatalytic process is added to every caspase reaction.

By using the apoptosis scheme modeled as an HFPN, we simulated the DNA fragmentation amount by varying the Fas ligand concentration and Figure 11 shows the simulated relationship. It shows that under very weak stimulation (very low amount of Fas ligand), DNA fragmentation does not occur since the stimulation stops at the intermediate point because of the assumption of degradation processes. With the increase of the stimulation, the reaction proceeds to the backward intermediates and DNA fragmentation (cell death) occurs finally, which increases with the increase of the Fas ligand concentration.

There are two pathways from activated caspase 8 to caspase 3, one through several steps including the cytochrome c release from mitochondria when the concentration of activated caspase 8 is low, and the direct one to caspase 3 when the concentration of activated caspase 8 is high [20]. We assume arbitrarily that the direct pathway starts when the concentration of activated caspase 8 is larger than 30. Reportedly the removal of the Bid by gene knockout method increases the resistance of liver cell apoptosis by Fas ligand, while it does not affect the apoptosis of thymus and embryonic cells. If the second pathway is included to the scheme, DNA fragmentation increases slightly, especially, when the Fas ligand concentration is high (Figure 11). However the detailed mechanism of the selection of these two pathways from caspase 8 are still unclear and necessary to be studied in future in the laboratory.

Since the presence of autocatalytic process is proposed in caspases [21], it is included in our model (Figure 12), which increases the DNA fragmentation as shown in Figure 11. However, if the large rate of the autocatalytic process is assumed in the caspase reaction, the DNA fragmentation becomes independent of the Fas ligand concentration, which disagrees with the experimental results. Therefore, we can guess that autocat-

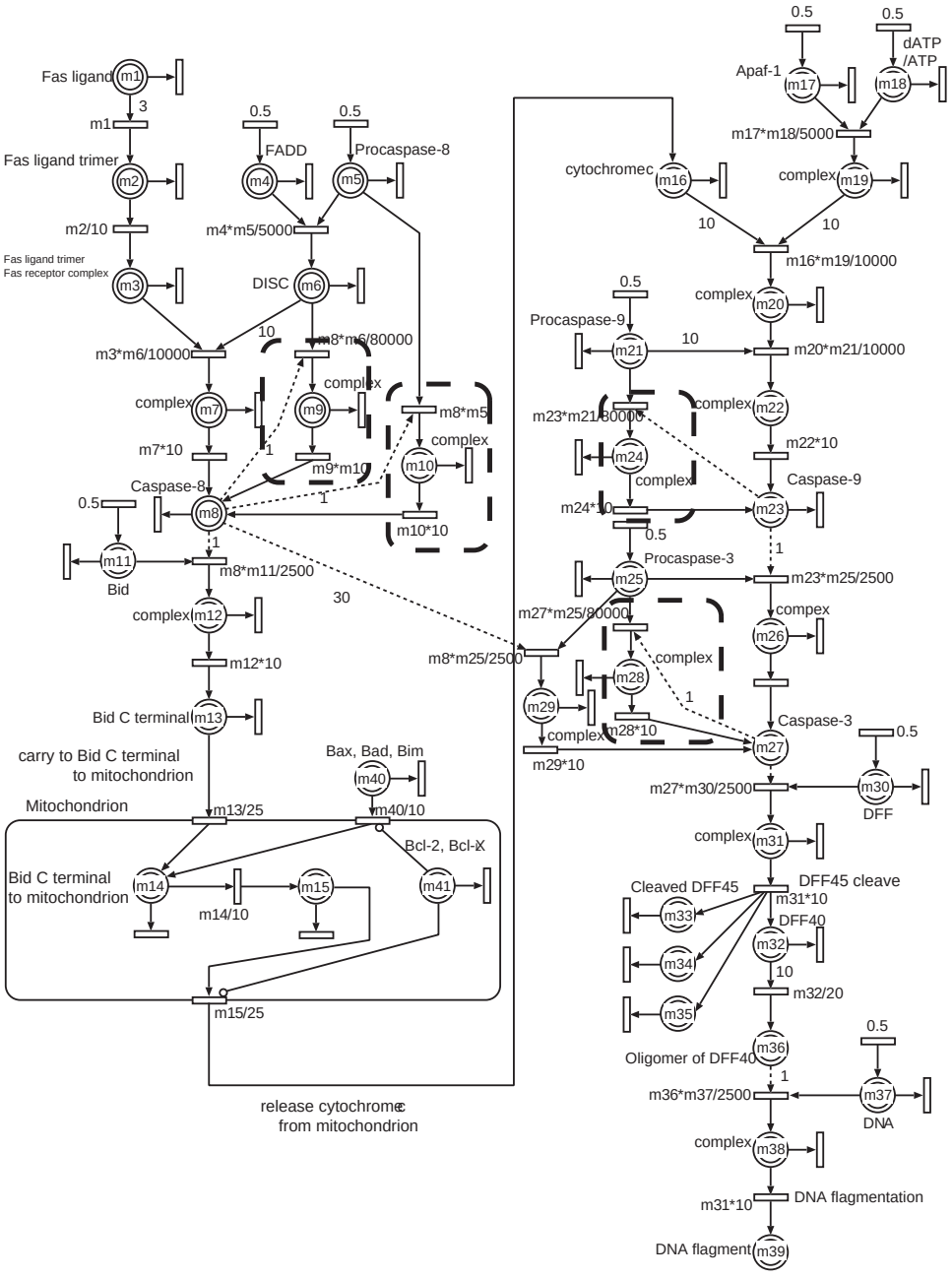

Figure 10: A HFPN representing the Fas-induced apoptosis by HFPN obtained from Figure 9. Autocatalytic processes (Figure 12) are surrounded by bold dotted lines. A HFPN file including all transition parameters can be downloaded from the URL $http://www.GenomicObject.Net$.

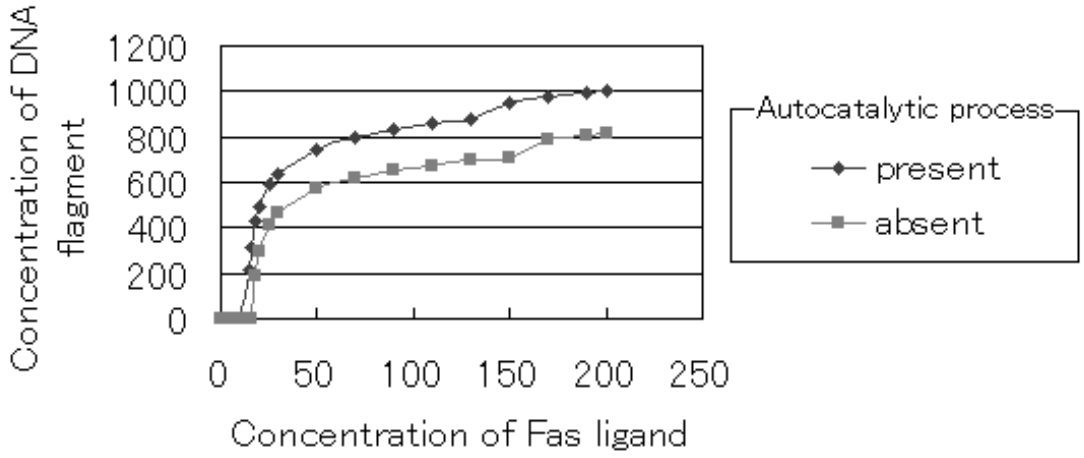

Figure 11: Simulated relationship between the DNA fragmentation amount and the Fas ligand concentration: At higher concentration of Fas ligand, the direct pathway from caspase 8 to caspase 3 contributes to the fragmentation. To examine the effect of autocatalytic process of caspases, DNA fragmentation is simulated for both cases of the presence and absence in this process.

Table 2: DNA fragmentation at four autocatalytic rates of caspases (rate0=0, rate1=$mA*mB/8000$, rate2=$mA*mB/4000$, and rate3=$mA*mB/2500$), which are assigned to the transition T_A in Figure 12. The stop time represents the period after that Fas ligand stimulation is stopped. The initial Fas ligand concentration is set to be $n = 200$. Variables mA and mB represent the contents of the continuous places going into T_A.

DNA Fragmentation				
Stop time	**rate0**	**rate1**	**rate2**	**rate3**
10	0	0	0	779
15	0	405	715	1824
20	402	567	869	2025

alytic processes must be slow if they are at present. To examine the effect of autocatalytic processes of caspases on the apoptosis by Fas ligand, DNA fragmentation is simulated when the stimulation by Fas ligand stopped after a short period. Table 4 shows a simulation result that the apoptosis proceeds more with the increase of the autocatalytic rate of caspases even for a short period stimulation.

Figure 13 shows simulated time courses of the HFPN in Figure 10 with *Genomic Object Net*. Some intermediates during apoptosis at three levels of Fas ligand concentrations are measured. These time courses might be useful to plan new experiments such as addition of inhibitors to some step. However, it is necessary to estimate the realistic rates of each reaction by the comparison with the experimental data. It is also necessary to add other pathways through Bcl-2 family or p53 to describe the real apoptosis held in various cells and by various inducers.

5 Conclusions

The effectiveness of HFPN based biopathway modeling is demonstrated through two examples of the circadian rhythm in *Drosophila* and the apoptosis induced by Fas ligand. Simulations of these models are performed on the software tool *Genomic Object Net* and some observations in biological aspects are obtained.

We have developed *Genomic Object Net Visualizer* (GON Visualizer) based of XML technology [22]. GON Visualizer allows us to visualize simulation results of *Genomic Object Net* which are exported as CSV files. With this tool users in biology/medicine can realize visualizations of simulation results of the aimed biological phenomenon by creating XML document in which CSV files produced by *Genomic Object Net* are included as

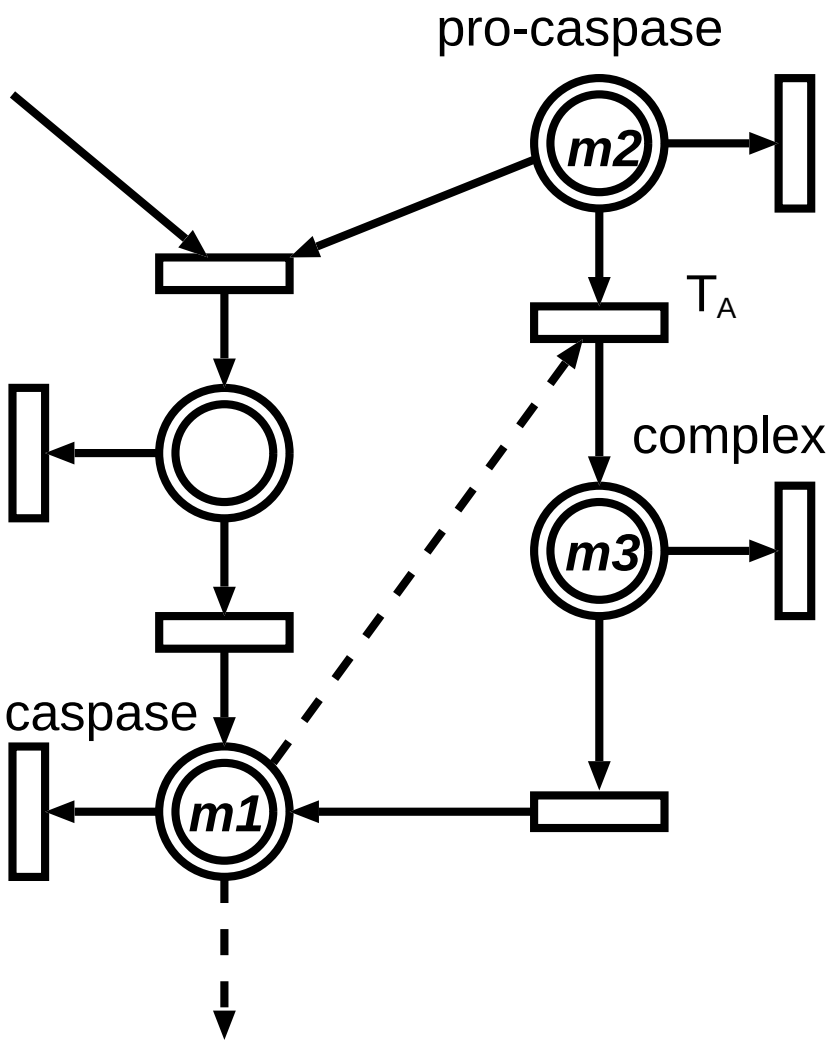

Figure 12: A HFPN representation of autocatalytic process in Figure 10.

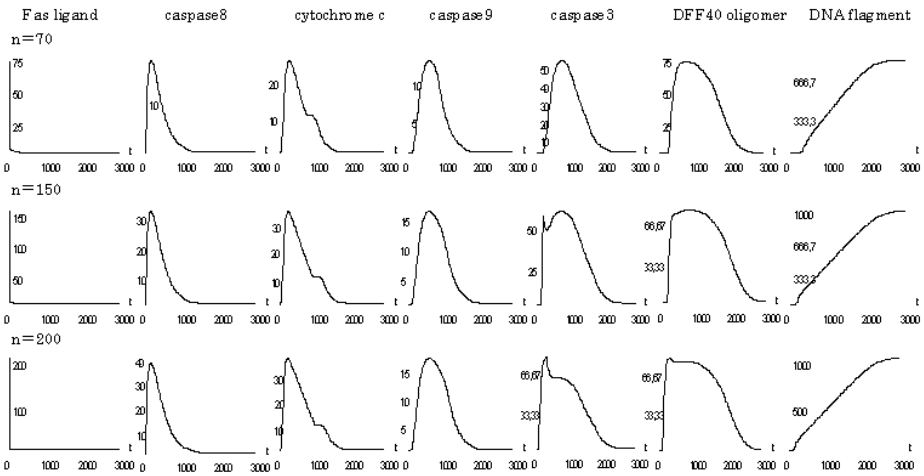

Figure 13: Simulated time courses of some intermediates during apoptosis for the Fas ligand concentration $n = 70, 150, 200$.

basic data for simulations. The visualizations of the biopathways introduced in this paper will be reported in the future.

Most of existing biopathways simulation tools only compute time courses of concentration behaviors of biological objects such as proteins and mRNAs. However, in general, distributions of these biological objects are not uniform because of compartmentalization. Thus, for more precise simulation, more complex informations such as localization of biological objects and molecular level cell-cell interaction should be included in simulation models. In order to address this problem, we introduced *hybrid functional Petri net with extension* (HFPNe) and developed "Genomic Object Net ver.1.0" based on the notion of HFPNe ($http://www.GenomicObject.Net$). One of features of HFPNe is that places of the HFPNe can have several types of data such as integer, real, boolean, string, and vector. With this feature, the HFPNe allows us to include the more complex biological information in computational biopathway models. We will demonstrate modeling methods for describing the computational biolpathway model with Genomic Object Net ver.1.0 in the near future.

References

[1] Mendes, P. (1993). GEPASI: a software for modeling the dynamics, steady states and control of biochemical and other systems. *Comput. Appl. Biosci.* **9(5)**, 563–571.

[2] Tomita, M., Hashimoto, K., Takahashi, K., Shimizu, T., Matsuzaki, Y., Miyoshi, F., Saito, K., Tanida, S., Yugi, K., Venter, J.C. and Hutchison, C. (1999). E-CELL:Software environment for whole cell simulation. *Bioinformatics* **15**, 72–84.

[3] Stelling, J., Kremling, A. and Gilles, E.D. (2000). Towards a virtual biological laboratory. *Foundations of Systems Biology, Kitano, H. (eds.)*. MIT Press, pp.189–212, 2000.

[4] Stokes, C.L. (2000). Biological systems modeling: powerful discipline for biomedical e-R&D. *AIChE J.* **46**, 430–433.

[5] Alla, H. and David, R. (1998). Continuous and hybrid Petri nets. *Journal of Circuits, Systems, and Computers* **8(1)**, 159–188.

[6] Valk, R. (1978). Self-modifying nets, a natural extension of Petri nets. *Lecture Notes in Computer Science* **62** (ICALP '78), 464–476.

[7] Drath, R. (1998). Hybrid object nets: An object oriented concept for modeling complex hybrid systems. *Proc. Hybrid Dynamical Systems, 3rd International Conference on Automation of Mixed Processes, ADPM'98*, 437–442.

[8] Drath, R., Engmann, U. and Schwuchow, S. (1999). Hybrid aspects of modeling manufacturing systems using modified Petri nets. *In: 5th Workshop on Intelligent Manufacturing Systems*. Granado, Brasil.

[9] Dunlap, J.C. (1999). Molecular bases for circadian clocks. *Cell* **96**, 271–290.

[10] Glossop, N.R.J., Lyons, L.C. and Hardin, P.E. (1999). Interlocked feedback loops within the *Drosophila* circadian oscillator. *Science* **286**, 766–768.

[11] Hardin P.E. (2000). From biological clock to biological rhythms. *Genome Biology 2000* **1(4)**, reviews1023.1-1023.5.

[12] Kloss, B., Price, J.L., Saez, L., Blau, J., Rothenfluh, A., Wesley, C.S. and Young, M.W. (1998). The *Drosophila* clock gene double-time encodes a protein closely related to human casein Kinase Iϵ. *Cell* **94**, 97–107.

[13] Price, J.L., Blau, J., Rothenfluh A., Adobeely, M., Kloss, B. and Young, M.W. (1998). double-time is a novel Drosophila clock gene that regulates PERIOD protein accumulation. *Cell* **94**, 83–95.

[14] Leloup, J-C. and Goldbeter, A. (1998). A model for circadian rhythms in *Drosophila* incorporating the formation of a complex between the PER and TIM proteins. *J. Biol. Rhythms* **13** (1), 70–87.

[15] Ueda, H.R., Hagiwara, M. and Kitano, H. (2001). Robust oscillations within the interlocked feedback model of Drosophila circadian rhythm. *J. Theor. Biol.* **210 (4)**, 401–406.

[16] Young, M.W. (2000). Marking time for a kingdom. *Science* **288**, 451–453.

[17] Jacobson, M.D., Weil, M. and Raff, M.C. (1997). Programmed cell death in animal development. *Cell* **88**, 347–354.

[18] Thompson, C.B. (1995). Apoptosis in the pathogenesis and treatment of disease. *Science* **267**, 1456–1462.

[19] Nijhawan, D., Honarpour, N. and Wang, X. (2000). Apoptosis in neural development and disease. *Annual Reviews of Neuroscience* **23**, 73–87.

[20] Kuwana, T., Smith, J.J., Muzio, M., Dixit, V., Newmeyer, D.D. and Kornbluth, S. (1998). Apoptosis induction by caspase-8 is amplified through the mitochondrial release of cytochrome c. *Journal of Biological Chemistry* **273**, 16589–16594.

[21] Hugunin, M., Quintal, L.J., Mankovich, J.A. and Ghayur, T. (1996). Protease activity of in vitro transcribed and translated Caenorhabditis elegans cell death gene (ced-3) product. *Journal of Biological Chemistry* **271**, 3517–3522.

[22] Matsuno, H., Doi, A., Hirata, Y. and Miyano, S. (2001). XML documentation of biopathways and their simulations in Genomic Object Net. *Genome Informatics* **12**, 54–62.